

Non-contact and Noise Tolerant Heart Rate Monitoring using Microwave Doppler Sensor and Range Imagery

Daichi Matsunaga, Shintaro Izumi, *Member, IEEE*, Keisuke Okuno, *Student member, IEEE*, Hiroshi Kawaguchi, *Member, IEEE*, and Masahiko Yoshimoto, *Member, IEEE*

Abstract—This paper describes a non-contact and noise-tolerant heart beat monitoring system. The proposed system comprises a microwave Doppler sensor and range imagery using Microsoft Kinect™. The possible application of the proposed system is a driver health monitoring. We introduce the sensor fusion approach to minimize the heart beat detection error. The proposed algorithm can subtract a body motion artifact from Doppler sensor output using time–frequency analysis. The body motion artifact is a crucially important problem for biosignal monitoring using microwave Doppler sensor. The body motion speed is obtainable from range imagery, which has 5-mm resolution at 30-cm distance. Measurement results show that the success rate of the heart beat detection is improved about 75% on average when the Doppler wave is degraded by the body motion artifact.

I. INTRODUCTION

Non-contact and remote biosignal measurement techniques offer great potential for healthcare applications. In contrast to traditional mobile or wearable healthcare devices, non-contact systems have fine usability: the most important factor to popularize healthcare devices. As described herein, we specifically examine a non-contact and non-invasive heart rate monitoring method. The heart rate and heart rate variability are useful indices for cardiac disease detection, stress monitoring, active mass monitoring, and so on.

Electrocardiography (ECG), the standard method of heart rate measurement, can be done even in daily life using a traditional Holter monitor or a wearable ECG sensor [1–3]. However, these devices should be pasted to a user's skin using uncomfortable electrodes. To mitigate the discomfort of electrodes, a capacitive coupling ECG sensor [4–5] and a photoplethysmographic sensor [6–7] have been developed. Although these devices can detect a heart rate without the need for adhesion, they should be near the human body. The possible application of the proposed system is a driver health monitoring.

To realize remote heart rate monitoring, a microwave Doppler sensor [8–14] has been proposed to detect the heart velocity. Imaging-based methods use the color change of the face, which indicates the pulse beat. Although these methods present severe noise contamination problems, the heart rate can be detected from tens of centimeters to several meters distance. For this work, we chose the microwave Doppler sensor as the remote heart rate monitor.

D. Matsunaga, S. Izumi, K. Okuno, H. Kawaguchi, and M. Yoshimoto are with the Graduate School of System Informatics, Kobe University, 1-1 Rokkodai, Nada, Kobe, Hyogo 657-8501, Japan (e-mail: matsunaga.daichi@cs28.cs.kobe-u.ac.jp).

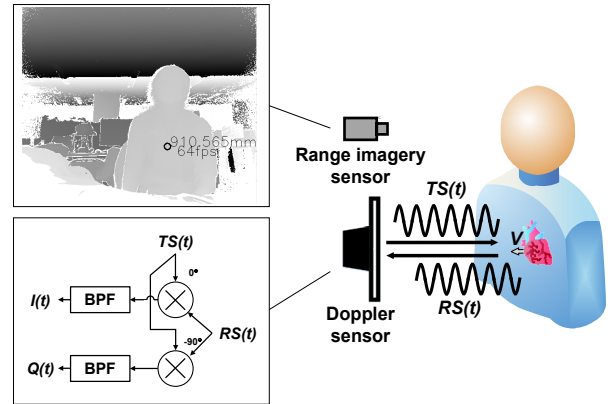


Fig. 1. Heart rate monitoring system using microwave Doppler sensor and range imagery.

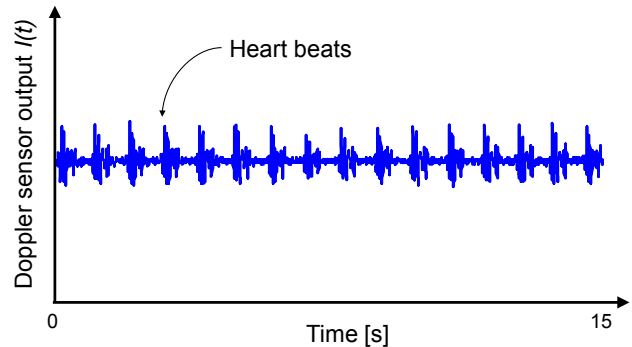


Fig. 2. Example of Doppler sensor output including heart beats.

The most important problem of the microwave Doppler sensor for heart rate monitoring is human body motion artifacts. Because a user is not always at rest in daily life, motion artifacts must be eliminated for home and daily use of this sensor. Therefore, we propose a noise reduction algorithm based on a sensor fusion approach using both the microwave Doppler sensor and range imagery simultaneously. Fig. 1 portrays the proposed system configuration.

II. HEART BEAT MONITOR USING MICROWAVE DOPPLER SENSOR

As presented in Fig. 1, the microwave Doppler sensor outputs Doppler waves $I(t)$ and $Q(t)$ by mixing a transmission wave $TS(t)$ and a received wave $RS(t)$. In this work, we employ a 24-GHz microwave sensor; only $I(t)$ is used to detect the heart beat. $I(t)$ can be derived from the following equation:

$$I(t) = \frac{AA'}{2} \sin\left(\frac{2V}{\lambda} \times 2\pi t\right). \quad (1)$$

Here A , A' , λ , and V respectively denote the transmitted wave amplitude, the received wave amplitude, the transmitted

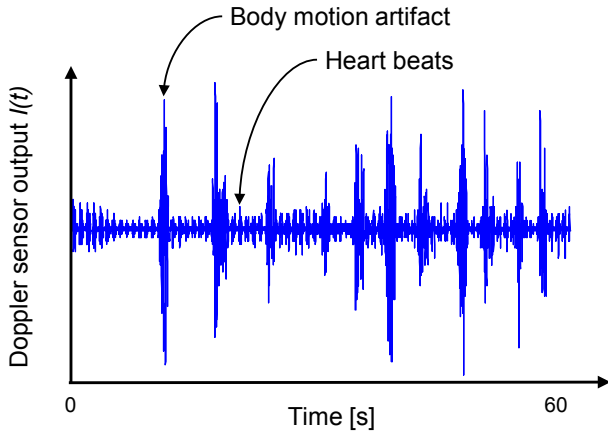


Fig. 3. Doppler sensor output with body motion artifact.

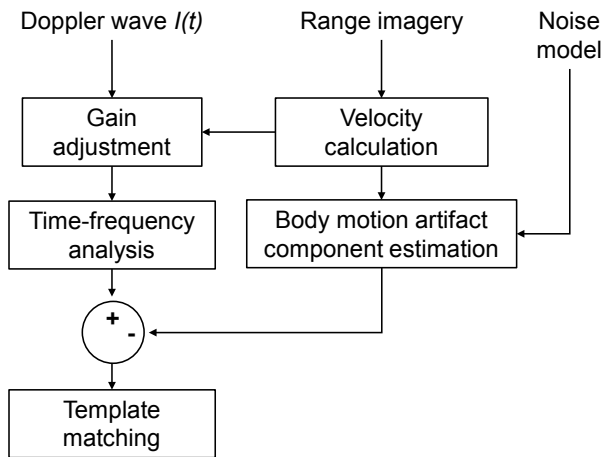


Fig. 4. Flow chart of body motion artifact reduction method.

wave wavelength, and the target object velocity (m/s). The difference between $Q(t)$ and $I(t)$ is $\pi/2$ phase delay. Although it is useful for direction estimation, only $I(t)$ is required in our system to detect the heart rate. When the microwave is irradiated to the chest of a subject in a resting condition, the Doppler wave $I(t)$ includes information of the heart beat velocity, as presented in Fig. 2. Therefore, the heart rate is obtainable from the Doppler wave $I(t)$.

In conventional works, time domain signal processing techniques are used to extract the heart rate from the Doppler wave. For example, short-term autocorrelation is used for extraction [14]. However, when the subject is not at rest, it is difficult to detect the heart beat correctly using the time domain analysis. When the subject moves, the Doppler wave $I(t)$ is contaminated by the velocity of the human body motion, as depicted in Fig. 3. We designate this noise as a body motion artifact. If the $I(t)$ includes both the velocity of the human body motion W and the velocity of the heart beat V , then it can be explained as shown below.

$$I(t) = \frac{AA'_1}{2} \sin\left(\frac{2W}{\lambda} \times 2\pi t\right) + \frac{AA'_2}{2} \sin\left(\frac{2(W+V)}{\lambda} \times 2\pi t\right). \quad (2)$$

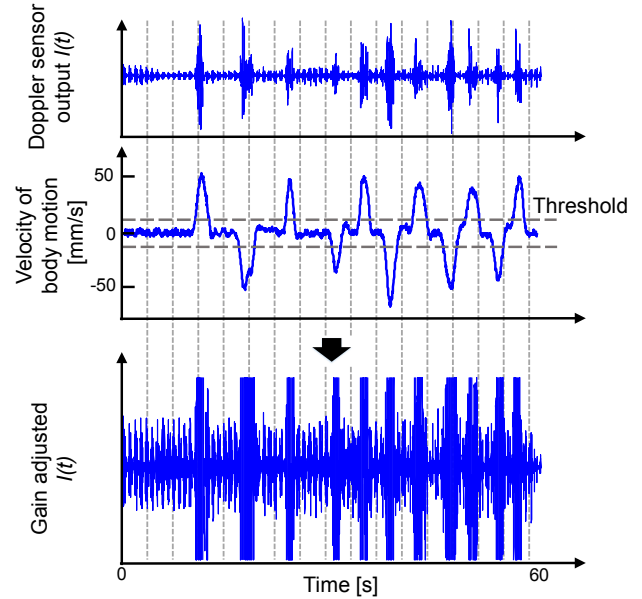


Fig. 5. Gain adjustment of Doppler signal with body motion artifact.

In this equation, the first term signifies the velocity component of whole body motion. The second term represents the velocity component of the heart beat. The heart beat velocity is offset by the body motion velocity.

III. NOISE REDUCTION ALGORITHM USING SENSOR FUSION TECHNIQUE

To eliminate the body motion artifact, we introduce a sensor fusion approach, which uses both a microwave Doppler sensor and range imagery as presented in Fig. 1. The range imagery obtained by Microsoft Kinect™ is used to estimate the body motion velocity using the change of the distance from the body surface. It has 5-mm resolution at 30-cm distance by averaging 121 pixels. Fig. 4 presents a flow chart of the proposed method.

A. Gain adjustment considering body motion artifact

First, we introduce an automatic gain adjustment method for Doppler wave. The amplitude of the reflected wave including heart beat components fluctuates attributable to the body motion or respiration of the subject. The gain of the fluctuation depends on the Doppler sensor frequency characteristics. To detect the heartbeat correctly, it is necessary to suppress this fluctuation by the gain adjustment.

Fig. 5 presents an example of gain adjustment. The measured Doppler output $I(t)$ is partitioned every 3.667 s, because at least one heartbeat component is comprised in this duration. Then, the peak-to-peak value of the Doppler output in each partition is calculated. However, if the body motion velocity is greater than a threshold, then the corresponding data of the Doppler output are excluded from the peak-to-peak calculation. The body motion velocity is calculated from the distance of the body surface, which is obtainable by averaging the 121 points of depth information around the chest from the range imagery. Then, the resolution of the gain of each partition is adjusted according to the peak-to-peak value. In this study, the velocity threshold is empirically set to 10 mm/s.

B. Time–frequency analysis using MEM

Next, a time–frequency analysis of the Doppler output is conducted using a Maximum Entropy Method (MEM) [15]. Because the Doppler wave $I(t)$ is contaminated by the complicated frequency components as shown in (2), it is difficult to eliminate the body motion artifact using only time domain processing. Therefore, we use the time–frequency analysis. The MEM can obtain an accurate frequency analysis despite the small sample size. This characteristic is beneficial for extracting heart beat components from the Doppler output including body motion artifact. Fig. 6(c) shows some results of time–frequency analysis using MEM. This result fundamentally obeys the assumed body motion artifact model in (2). Although the center frequency of the body motion artifact is lower than those of the heart beat components, they are partially overlapped still in the frequency domain because the body motion artifact has a wide frequency range.

C. Body motion artifact reduction in frequency domain

We create the noise model in (2). However, the body motion velocity is not a constant. Also, its spectrum is distributed in the lower frequency range overlapping the heart

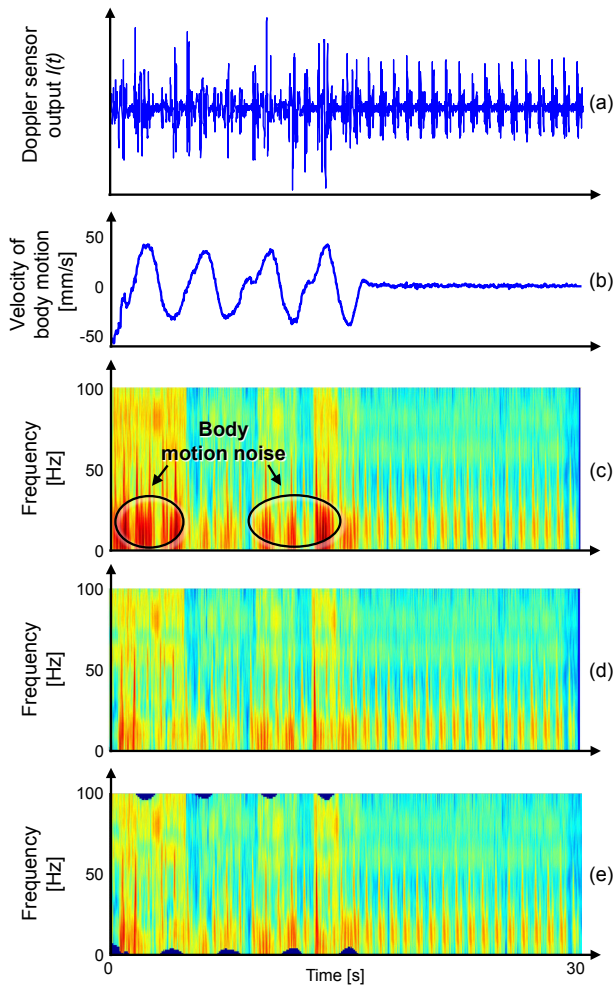


Fig. 6. Example of time–frequency analysis using MEM and body motion artifact reduction; (a) measured Doppler sensor output, (b) velocity information from range imagery, (c) spectrogram of Doppler sensor output using MEM, (d) spectrogram after noise reduction, and (e) spectrogram after frequency shift.

beat components. To eliminate the body motion artifact, this component is extracted from the time frequency analysis result. We choose the power spectrum as a baseline without heart beat and motion artifact components. The body motion artifact component can be extracted by subtracting the baseline and the power spectrum including the body motion artifact. These power spectra can be selected using velocity information. Body motion affects the gain and the center frequency of the body motion artifact component velocity, but their relation can be estimated from the Doppler sensor frequency characteristics. Therefore, the body motion artifact component can be modeled easily as a function of the body motion velocity.

Fig. 6 presents an example of the body motion artifact reduction using a result of time–frequency analysis and the velocity information. The result shows that the body motion artifact component is suppressed. Nevertheless, the center frequency of several heart beat components in the high velocity range is shifted, as shown in the second term of (2). It can also be fixed by shifting to the inverse direction according to the velocity information, as depicted in Fig. 6(e).

D. Template matching in time–frequency domain

Finally, the heart beat intervals are extracted to calculate the heart rate. Then, we use a template matching algorithm [16], which can extract a similar wave form robustly from noisy measured signals. We extend this algorithm to the time–frequency range.

IV. PERFORMANCE EVALUATION

A. Measurement method

To evaluate the proposed system and algorithm, we measured the Doppler wave, range imagery, and the heart rates for three male subjects aged 22–23. The measurement duration was 30 s. Fig. 7 presents the experimental setup. The subjects were measured in a sitting posture because we assumed an in-vehicle system application. All subjects were measured at rest and with body motion conditions.

Distance between the subject and the range imagery sensor (Microsoft Kinect for Windows v2; Microsoft Corp.) was set to 80 cm. The microwave Doppler sensor (NJR4232K1; New Japan Radio Co. Ltd.) was also set to 30-cm distance from the subject. An accurate heart rate was recorded simultaneously using an adhesive patch type ECG sensor (Actiwave Cardio; CamNtech) for use as a reference for performance evaluation. The required computational time to extract heart rates from the Doppler sensor output with 30 s duration is 6.32 s on average.

B. Measurement results

Fig. 8 shows measured waveforms and the heart rate extraction result of one subject with the body motion condition. The extracted heart rate was compared with the reference value of ECG sensor and the extracted value using a conventional method, which extracts the heart rate from the time-domain Doppler signal using template matching. Measurement results show body motion artifact suppression. The proposed method correctly extracted the heart rate.

Fig. 9 presents a comparison of the heart rate extraction success rate with three subjects. All of the extracted heart rate is compared with the logging data of the reference ECG sensor.

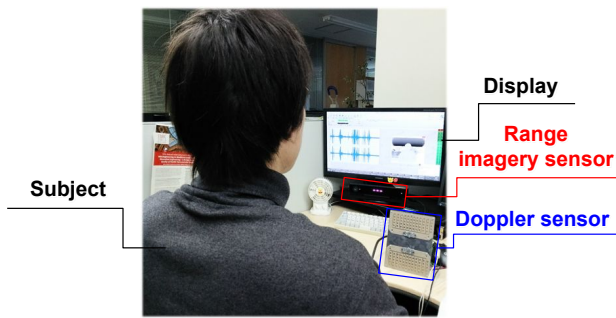


Fig. 7. Experimental setup.

The acceptable error range is set to $\pm 5\%$ in this work. Here, Conv. stands for the conventional time-domain template matching. Prop. 1 uses time–frequency domain analysis and template matching without velocity information. Prop. 2 includes all noise reduction method using velocity information. As shown in Fig. 9, the heart rate extraction success rate is improved in all conditions. The success rate is improved even in a resting condition by virtue of time–frequency domain processing. The success rate with the body motion artifact condition was improved about 75%, on average.

V. CONCLUSION

We proposed a sensor fusion approach to realize a non-contact and non-invasive heart rate monitoring system using the microwave Doppler sensor and the range imagery. The proposed method uses time–frequency analysis and body motion artifact reduction according to the velocity information of the body surface, as obtained using range imagery. The measurement results for three subjects in a non-rest condition show that the proposed method achieves 75% heart rate extraction success rate improvement, on average.

REFERENCES

- [1] K. Youngsung and C. Il-Yeon, "Wearable ECG Monitor: Evaluation and Experimental Analysis," *International Conference on Information Science and Applications (ICISA)*, pp. 1–5, April 2011.
- [2] K. Hsein-Ping and J. Do-Un, "Wearable patch-type ECG using ubiquitous wireless sensor network for healthcare monitoring application," *Proc. of the Second International Conference on Interaction Sciences*, pp. 624–630, Nov. 2009.
- [3] C. Xianxiang, Xinyu Hu; R. Ren, Z. Bing, T. Xiao, X. Jiabai, F. Zhen, Q. Yangmin, L. Huaiyong and T. Lili, X. Shan hong, "Noninvasive Ambulatory Monitoring of the Electric and Mechanical Function of Heart with a Multifunction Wearable Sensor," *Proc. of IEEE COMPSACW*, pp. 662–667, July 2014.
- [4] D. Shao, Y. Yang, C. Liu, F. Tsow, H. Yu and N. Tao, "Noncontact Monitoring Breathing Pattern, Exhalation Flow Rate and Pulse Transit Time," *Proc. of IEEE Transactions on Biomedical Engineering*, vol. 61, no. 11, pp. 2760–2767, November 2014.
- [5] D. McDuff, S. Gontarek and R.W. Picard, "Improvements in Remote Cardiopulmonary Measurement Using a Five Band Digital Camera," *Proc. of IEEE Transactions on Biomedical Engineering*, vol. 61, pp. 2593–2601, no. 10, October 2014.
- [6] L. Bor-Shyh, W. Chou, W. Hsing-Yu, H. Yan-Jun and P. Jeng-Shyang, "Development of Novel Non-Contact Electrodes for Mobile Electrocardiogram Monitoring System," *Proc. of IEEE Translational Engineering in Health and Medicine*, pp. 1–8, 2013.
- [7] Y.M. Chi, S.R. Deiss and G. Cauwenberghs, "Non-contact Low Power EEG/ECG Electrode for High Density Wearable Biopotential Sensor Networks," *Sixth International Workshop on Wearable and Implantable Body Sensor Networks*, pp. 246–250, June 2009.

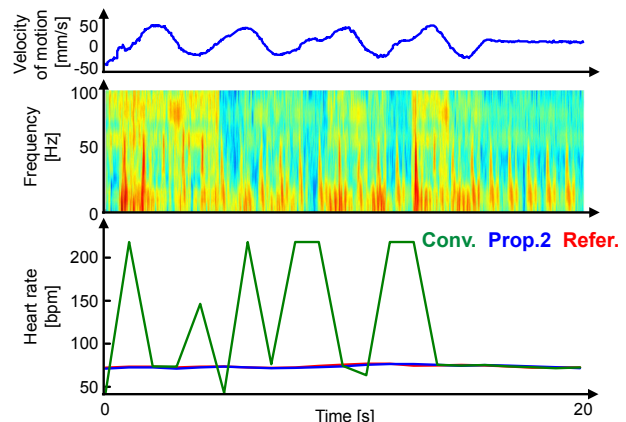


Fig. 8. Measurement result of heart rate extraction and comparison with reference sensor and conventional method.

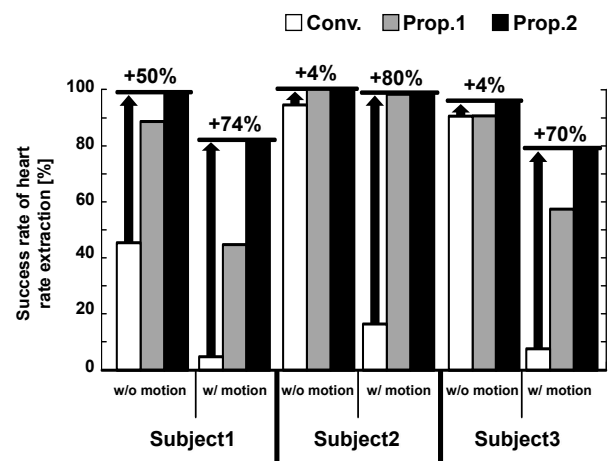


Fig. 9. Measurement results of heart rate extraction success rate.

- [8] A. Tedim, P. Amorim and A. Castro, "Development of a System for the Automatic Detection of Air Embolism Using a Precordial Doppler," *Proc. of IEEE EMBC*, pp. 2306–2309, August 2014.
- [9] A.K. Tafreshi, M. Karadas, C.B. Top and N.G. Gencer, "Data Acquisition System for Harmonic Motion Microwave Doppler Imaging," *Proc. of IEEE EMBC*, pp. 2873–2876, August 2014.
- [10] J.P. Phillips and P.A. Kyriacou, "Comparison of methods for determining pulse arrival time from Doppler and photoplethysmography signals," *Proc. of IEEE EMBC*, pp. 3809–3812, August 2014.
- [11] S. Kogelenberg, C. Scheffer, M.M. Blankenberg and A.F. Doubell, "Application of laser Doppler vibrometry for human heart," *Proc. of IEEE EMBC*, pp. 3809–3812, August 2014.
- [12] C.B. Top, A.K. Tafreshi and N.G. Gencer, "Harmonic Motion Microwave Doppler Imaging Method for Breast Tumor Detection," *Proc. of IEEE EMBC*, pp. 6672–6675, August 2014.
- [13] D. Obeid, S. Sadek, G. Zaharia and G.E. Zein, "Feasibility Study for Non-Contact Heartbeat Detection at 2.4 GHz and 60 GHz," *International Union of Radio Science (URSI)*, 2008.
- [14] D. Nagae and A. Mase, "Measurement of heart rate variability and stress evaluation by using microwave reflectometric vital signal sensing," *Proc. of AIP Review of Scientific Instrument*, vol. 81, no. 9, pp. 0943011–0943014, September 2010.
- [15] The Maximum Entropy Method (MEM) of Data Analysis <http://cmm.cit.nih.gov/maxent/letsgo.html>
- [16] Y. Nakai, S. Izumi, M. Nakano, K. Yamashita, T. Fujii, H. Kawaguchi and M. Yoshimoto, "Noise Tolerant QRS Detection using Template Matching with Short-Term Autocorrelation," *Proc. of IEEE EMBC*, pp. 6672–6675, August 2014.